BEAM LOSS MONITORING FOR DEMANDING ENVIRONMENTS

E. B. Holzer*, CERN, Geneva, Switzerland

Abstract

Beam Loss Monitoring (BLM) is a key protection system for machines using beams with damage potential and is an essential beam diagnostic tool for any machine. All BLM systems are based on the observation of secondary particle showers originating from escaping beam particles. With ever higher beam energies and intensities, the loss of even a tiny fraction of the beam can lead to damage or, in the case of superconducting machines, quenches. Losses also lead to material aging and activation and should therefore be well controlled and reduced to a minimum. The ideal BLM system would have full machine coverage and the capability to accurately quantify the number of lost beam particles from the measured secondary shower. Position and time resolution, dynamic range, noise levels and radiation hardness all have to be considered, while at the same time optimizing the system for reliability, availability and maintainability. This contribution will focus on design choices for BLM systems operating in demanding environments, with a special emphasis on measuring particle losses in the presence of synchrotron radiation and other background sources.

INTRODUCTION

A Beam Loss Monitoring (BLM) system has three main roles: provide protection against beam induced damage or quench, provide a diagnostics tool for the operation and commissioning of the machine, and keep the activation levels low. When beam particles in an accelerator or a transfer line deviate from the ideal trajectory, they eventually hit the vacuum chamber walls or beamline components and generate secondary particle showers. If their energy is high enough to penetrate, these secondaries can be measured outside of the machine by a BLM system. Hence, for all but the very lowest energy machines, beam loss monitoring is an essential beam diagnostics tool. It applications include: beam steering in linear machines, by minimizing the losses along the line; diagnostic of failure scenarios; search for aperture restrictions or erroneous machine elements causing local losses.

It is important to minimize beam losses even if they are not immediately compromising the machine structure, as they lead to aging of the materials and to activation. Radiation levels have to be kept as low as possible to limit human exposure during maintenance and repair work and to reduce the amount and activation levels of radioactive material at the end of the machine life-cycle. Collimation systems play an important role in this respect. They concentrate the unavoidable losses in comparatively short regions and, in the ideal case, can keep the rest of the machine virtually loss free. The importance of beam collimation increases at very high beam intensities and energies, where uncontrolled losses of even the beam halo have to be avoided.

The first part of the paper will discuss general design considerations for a BLM system with a focus on machines with damage potential, on regions of high radiation levels and on physically large machines. Machine protection, the coverage of loss scenarios and the system dependability will be discussed, as well as the possibility to resolve the position, the magnitude and the time structure of the losses. The second part of the paper discusses background sources to the beam loss measurement. These can limit the sensitivity, reduce the dynamic range and even compromise the machine protection functionality. Showers from distant beam losses, radiation from accelerating structures and background due to synchrotron radiation are reviewed. Throughout the paper examples will be given mostly of recent and current developments to cope with the challenges of future machines.

BLM FOR MACHINE PROTECTION

Where the beam has the potential to damage accelerator structures or to cause quenches in superconductive machines, by far the most demanding role of the BLM system is machine protection. On October 9, 2015 the record level of 200 MJ of stored energy per beam was surpassed with 6.5 TeV beams in the LHC as part of the intensity ramp-up. 362 MJ per beam is envisaged at the design beam energy of 7 TeV and nominal beam intensity. Already one LHC pilot bunch of 5×10^9 protons is close to the damage limit at 7 TeV. At HL-LHC (High Luminosity LHC), a major upgrade of the LHC planned for 2023, it is foreseen that the energy of one beam will reach 694 MJ, and even 8 GJ is envisaged for FCC-hh (Future Circular hadron Collider). Besides the beams, the enormous amount of 10 GJ will be contained in the LHC magnets at 7 TeV. This corresponds to 2.4 ton of TNT. If even a small fraction of this energy is released in an uncontrolled way massive damage could result.

In the design of the CLIC (Compact Linear Collider) two beam module, a low energy (2.4 GeV) and high current (100 A) electron drive beam is decelerated and the extracted power is transferred to a high energy (1.5 TeV) and low current (1.2 A) electron or positron main beam. The nominal beam power is large, 72 MW and 14 MW for the drive and the main beam respectively. Losses from either beam can have severe consequences. The most critical beam quantities are the high intensity for the drive beam and the high energy and small emittance for the main beam.

A powerful machine protection system is vital for all machines with damage potential and constitutes an integral part of the machine design. The BLM system is one of its key components. When losses exceed threshold values on any one of the 3600 loss detectors at the LHC, the beam is safely aborted. The thresholds depend on the detector location, the

_____
barbara.holzer@cern.ch

beam energy and the duration of the loss (in a range of 40 μs – 84 s), resulting in a total of about 1.5 million threshold values which span up to eight orders of magnitude. The CLIC machine protection is based on a 'next cycle permit': A subsequent injection is inhibited, when the onset of a potentially dangerous loss is detected.

A dependability analysis comprising reliability, availability, maintainability and safety is required for the design of a machine protection system. This analysis yields the allowed budgets for the BLM system in terms of: probability of component damage due to malfunction; downtime due to false alarms; and downtime due to maintenance. There is an inherent conflict between these budgets. By reducing the damage probability (hence increasing the protection) the machine availability will go down due to increased numbers of false dumps and maintenance time.

DETECTOR CHOICE AND DISTRIBUTION

BLM systems employ either a number of individual, localized particle detectors (e. g. pin diodes, short ionization chambers) installed at likely loss locations such as aperture limitations, or long distributed detectors (e. g. fibers, RF cables) covering the whole beamline.

Individual, Short Particle Detectors

Typical locations for loss monitors include: quadrupoles; collimators, scrapers and masks; stripping or charge exchange foils; aperture restrictions for dispersive particles; beam dump regions; injection and extraction regions; beam diagnostics posing an aperture restriction e. g. mirrors, or utilizing gas injection.

For the best time resolution, a very small detector is required. Diamond BLMs at selected locations in the LHC have a time resolution of a few ns and give a one turn bunch-by-bunch loss measurement [1, 2]. Experience at the LHC shows that a significant localized loss anywhere in the machine leads to losses at the primary collimators as well. Hence, the time structure of the loss can be resolved by just a few high resolution BLMs at the collimators [3].

Small crystal Cherenkov detectors coupled to fast photon sensors have the potential to achieve even higher time resolution. Since Cherenkov light emission is a prompt process, the time resolution is governed by the size and the refractive index of the radiator and the photon sensor performance. With current sensor technologies, which in the sensitivity range of interest approach the 100 ps range, intra-bunch loss measurements at the LHC should be feasible.

The position resolution is given, in general, by the distance between the installed detectors. For the same magnitude of loss (same number of lost beam particles), the measured signal varies strongly with the distance from the detector. For the LHC it has been simulated that this can easily reach a factor of ten for only one meter. If, however, the loss is visible on several detectors, a much more precise loss location and magnitude can be determined with the help of detailed shower simulations [4]: FLUKA [5, 6] simulations based on detailed models of the LHC have been estimated to determine the position of losses caused by beam-dust particle interactions to within ± 1 m and the number of inelastic proton-nucleus interaction in the event to within a factor of 2. The analysis of LHC magnet quenches during Run1 showed that, with good knowledge of initial conditions and sufficient data for validation, particle-tracking and particle-shower simulations provide, in the best cases, 20 % agreement of magnet model predicted quench levels with BLM signals in the region of peak losses [7]. For well known impact location and conditions (e. g. at a collimator or charge exchange foil) a conversion factor from BLM signal to impacting particles can be determined by measurement and/or simulation.

But all loss locations can not necessarily be predicted at the design stage. At the LHC, about one third of the BLMs had to be relocated between Run1 and Run2, 2013–2014, to cover the circumference of the machine more uniformly. During beam operation previously unconsidered beam losses, dubbed 'UFO' losses, had appeared in high numbers all along the machine, also in the cold dipole magnets which had not been equipped with BLMs during Run1. These losses are believed to be caused by interactions of the beam with dust particles. At the 2015 LHC energy of 6.5 TeV they can quench a magnet. During Run1 no magnet quench due to an UFO event occurred. Less heat was deposited in the coils due to the lower beam energy, and the lower magnetic field meant a higher margin for coil heating. The BLM thresholds during Run1 were set conservatively at one third of the assumed quench level. In 2015, the thresholds were set right at the quench level as calculated and measured during quench test campaigns for arc and dispersion suppressor magnets. Three UFO induced quenches and nine BLM protection dumps without quench occurred till October 4, 2015 in these regions . The now better longitudinal coverage due to BLM relocation allowed to increase the beam abort thresholds by a factor of 30, as the variation in measured BLM signal at the magnet quench level due to position variations is reduced.

Distributed, Long Particle Detectors

Long, distributed loss detectors avoid holes in the coverage. They are of particular interest for large machines and for beams of high damage potential. The number of monitors and readout channels is significantly reduced, lowering the cost and easing the dependability requirements for the individual channel. Examples are long ionization chambers (e. g. gas filled coaxial RF cables), scintillator fibers and detection based on the Cherenkov effect in optical quartz fibers. They have successfully been employed on many machines for qualitative loss measurements.

BLM systems based on optical fibers have become increasingly popular in recent years in particular for electron machines that produce high levels of synchrotron radiation, see for example [8–11]. Beam loss induced high energy charged particles crossing an optical fiber generate Cherenkov light that is partially trapped and transported to the end, where a

photon sensor converts it into an electrical signal. The fibers are small, insensitive to photons and electromagnetic fields and can be adapted to a wide dose range by choosing appropriate combinations of fiber and readout. The measurement of the total dose deposited in the fiber, typically proportional to the amount of beam losses, requires full understanding of the system: Light generation and propagation, attenuation effects, optical coupling efficiencies and response of the photon sensor. Moreover, the aging of optical fibers in different irradiation conditions needs to be investigated and corrected by calibration. One fiber can cover up to approximately 100 m of beam line with a single detector, the range being limited by attenuation in the fiber. A time resolution of about 1 ns can be achieved and single bunch position resolutions down to 50 cm have been reported [10]. Because of attenuation effects the measured signal height and the loss location (distance to the photo-detector) are coupled. For short beams the loss magnitude can be determined by applying an appropriate calibration. To be able to use fiber loss detectors for machine protection, further R&D work is required, in particular for absolute loss measurements and for position and time resolution of long bunch trains.

A straight forward absolute longitudinal position and time measurement can be achieved with long detectors whenever the combination of bunch spacing, beam velocity, detector length and traveling time of the signal to the readout combines in a way that the loss signal of individual bunches never overlap at the readout, wherever the loss occurs along the detector. For long bunch trains this will, in general, not be the case any more. Time, position and loss magnitude information are coupled, and the reduced number of readout channels means that a general unfolding is not possible. Combination with a small detector with high time resolution measurement could help to recover also the position information. But most of the losses encountered during the life-time of a machine will be among a set of, eventually, well known loss scenarios. Once the scenarios are studied and cataloged it should be possible to analyze automatically the type and magnitude of the loss, recovering at the same time the position and time information. In a similar way, once the UFO loss pattern at the LHC was understood, it was possible to automatically detect these type of losses by combining the information from several monitors (locally and at the collimation) for online monitoring and statistical analysis.

Simulation studies of 100 m long Cherenkov fibers have shown a longitudinal resolution of 1 m and a time resolution of about 1 ns for the starting point of individual loss locations affecting all bunches in a long beam [12, 13]. First results from measurements at the Australian Synchrotron and the CLIC Test Facility (CTF3) indicate the feasibility of a position measurement for such loss scenarios with a resolution below 2 m [14].

MACHINE SIZE AND RADIATION

Physically large machines (like LHC, ILC, CLIC, FCC, SppC) pose considerable challenges for the BLM system already by their size alone. If localized detectors are chosen, their number increases in proportion to the number of optics cells. The cost increases, but also system maintenance and availability become increasingly challenging. More measurement data is produced, which needs to be extracted, logged, monitored, analyzed and made available for various online and offline applications. To keep electromagnetic interferences small, and considering the long distances involved, the front-end read-out electronics will in general be positioned in the accelerator tunnel, as close to the detector as feasible. In this case it has to be radiation tolerant, which considerably complicates design and production. Radiation certified components are often not available, therefore the radiation hardness has to be tested with particle beams. It is important to note, that only components from the same batch as the ones tested can be considered to have the corresponding radiation tolerance. Production details often change from batch to batch, influencing the susceptibility to radiation.

Example: Radiation Tolerant BLM ASIC

The LHC BLM front-end electronics is verified to be radiation tolerant up to 500 Gy. This is sufficient for the virtually loss free arcs even for the HL-LHC upgrade, where the electronics is placed in the vicinity of the detectors underneath the quadrupole magnets. The front-end electronics of the higher radiation dispersion suppressors and straight sections is placed up to 300–800 m away in radiation shielded locations. The long cables lead to increased noise levels, which are in some cases reaching the required beam abort levels for quench protection at 7 TeV. Development is ongoing to implement the front-end electronics in a radiation hard Application Specific Integrated Circuit (ASIC) [15, 16]. Again based on current-to-frequency conversion, it is packaged in a compact and radiation tolerant form. The plan is to install it directly on the ionization chamber, inside the so called electric box, which houses high voltage filtering. The integration time remains 40 µs. The dynamic range increases to 120 dB (40 fC – 42 nC) and it will newly operate with positive and negative input currents. The radiation tolerance up to 100 kGy has been verified using X-rays of 20 keV peak energy.

To transport the signal to the surface requires low noise, low loss signal transmission. Optical signal transmission and, in general, optical diagnostic techniques are preferable under such conditions.

BACKGROUND FROM DISTANT BEAM LOSSES

Collimation regions, the vicinity of the interaction points, regions of beam injection and beam extraction have particularly high levels of radiation. This poses a problem for beam loss monitoring, as a typical loss monitor cannot distinguish

between a beam loss and other sources of radiation. These additional radiation sources are often generated by beam losses further upstream (e. g. by collimation or scraping), losses from another beam line (injection or extraction lines, opposite beam in particle colliders), or by beam-beam collision products from interaction points. Critical regions in the LHC are the injection regions, which see losses from the injection line collimators; the collimation regions, which see losses from several collimators from the same beam and the opposite beam; and the insertion region triplet magnets, which are exposed to high radiation levels from collision debris.

Example: The CLIC Two-Beam Module

A particular case is the CLIC main linac, where the drive beam and the main beam run in parallel just 65 cm apart. The energy ranges from 2.37 to 0.237 GeV in the drive beam, and from 9 to 1500 GeV in the main beam. Beam dynamics considerations impose the total losses to be no more than 10^{-3} of the respective total beam intensity along the 20 km main linac as well as along each drive beam decelerator section. Otherwise, luminosity losses from beam loading variations would become intolerably high. Due to the large differences in beam intensity and energy the signal of the maximum acceptable loss of the main beam is up to two orders of magnitude below the signal of the maximum acceptable loss of the drive beam in the same two-beam module, for detector positions close to the respective quadrupole [17]. Due to the vicinity of the two beams, it is not obvious how to measure a main beam loss in the presence of a drive beam loss. For machine protection purpose that is actually not a problem, as simulations have shown that dangerous beam losses will be detected in any case.

An experiment was set up at the two-beam module of CTF3 to address the question of distinguishing the origin of the loss using Little Ionization Chambers (LIC), a shortened version of the LHC-type ionization chamber with only one signal electrode, and Cherenkov fiber detectors [18]. A first, limited measurement period showed losses on one beam leading to signals in the detectors on the other side of the two-beam module of 1–5 % of the signals on the side affected by losses. More systematic measurements will be performed.

Example: Cryogenic BLM for HL-LHC

Conventional loss detectors are installed on the outside of the magnets. At the LHC, the ionization chambers are located outside of the magnet cryostat, far from the superconducting coils. With the magnet yoke and the cryostat material in between, they can only measure the tails of the beam loss induced shower which heats the coils. The dose at the sensitive superconductor coil is much higher than the dose at the detector. The opposite is true for any background radiation from outside of the magnet: The cryostat and yoke now shield the coil and the dose to the detector will be higher than the dose to the coil. This effect can seriously hamper the loss measurement and compromise the quench protection.

The insertion region triplet magnets focus the beams on the interaction point. They are particularly challenging magnets, due to the high gradient of 215 T/m [19], their wide aperture and their exposure to a high radiation dose just 23 meters from the interaction point.
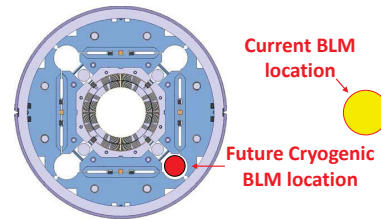

Figure 1: Cross section of the triplet magnet (MQXF) foreseen for HL-LHC, indicating the current BLM placement and the possible location of a cryogenic BLM [20].

For the HL-LHC upgrade it is foreseen to install loss detectors inside the new triplet magnets in super-fluid helium, see Fig. 1. Much closer to the loss location and shielded from other radiation sources, quench protection can be assured even in particularly high radiation areas. The system challenges include: operation of the detector in liquid helium at 1.9 K with a total radiation dose of 2 MGy during 20 years without access to the cold part of the system; a magnetic field of 2 T; fast pressure rise in case of magnet quench from 1.1 bar to 20 bar; a linear response in the range of 0.1 to 10 mGy/s; and the possibility to reliably predict and correct for radiation induced response degradation. The installation inside of the cryostat calls for very high dependability of the systems. Three different technologies are being investigated at CERN: liquid helium, silicon detectors and single crystal Chemical Vapour Deposition (scCVD) diamond detectors. The operation at such extreme conditions has not been previously attempted. Therefore, an extensive measurement program is being carried out at CERN since 2011 [20–22].

The liquid helium detector prototypes [21] were parallel plate ionization chambers, similar in design to the LHC-type ionization chamber, but smaller and with a plate distance of 1–3 mm. They can use directly the magnet cooling helium as ionization medium. With a full metal and ceramics design and the ionization medium being continuously flushed, this detector is intrinsically radiation hard. The detectors were tested at 1.8 and 4.2 K and up to 400 V/mm. The test measurements were promising, but not fully conclusive. In any case, the time resolution is limited by the low charge mobility in the order of 8–10 mm^2/Vs at 1.8 K [23], which is seven orders of magnitude smaller than the charge mobility in silicon at this temperature. The detector can not protect against losses which are faster than 180 µs. Hence it is too slow for the protection of the triplet magnets.

The behavior of the solid state detectors has been classified in terms of: detector sensitivity, leakage current, signal speed, signal shape, and radiation induced degradation of these parameters; and the dependency of the above on temperature, temperature cycling, bias voltage and dose rate. A variety of silicon and scCVD diamond detectors from differ-

ent manufacturers and with varying designs are investigated. The FWHM signal from a MIP (Minimum Ionizing Particle) at 1.9 K is 2.5 ± 0.7 and 3.6 ± 0.8 ns for silicon and diamond detectors respectively. This allows for bunch-by-bunch loss measurements. It could be shown that both materials can operate at 1.9 K and after irradiation of 2 MGy [22]. At liquid helium temperatures, the major downside of silicon compared to diamond, namely its high leakage current, disappears. The leakage current of an irradiated silicon detector remains below 100 pA at 400 V, even under forward bias. Figure 2 shows results for a 500 μm thick diamond with an active area of 22 mm^2 and gold metallization and a 300 μm p$^+$-n-n$^+$ silicon with an active area of 23 mm^2, aluminum metallization and a resistivity of 10 kΩ cm and 500 kΩ cm respectively. For low doses the sensitivity of the silicon is higher, but for high doses the diamond detectors give higher signals. With a decrease by a factor of 14 ± 3, the diamond shows the lowest signal degradation for a dose of 2 MGy. The expected signal degradation for silicon is of a factor of 25 ± 5. For absolute loss measurement and for machine protection, in any case, it is essential to establish a calibration method.
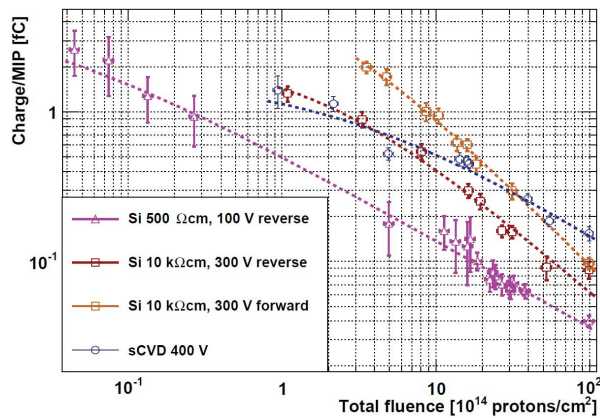

Figure 2: Radiation induced degradation of silicon and diamond detectors for a dose corresponding to 20 year of LHC operation in the triplet magnets [21].

Cryogenic BLMs were installed at the LHC to test the validity of the set-up and the long term behavior in the machine environment [24]. Two dipole magnets were equipped with four detectors each (one 500 μm scCVD diamond, one 100 μm silicon and two 300 μm silicon detectors) mounted right against the outside of the cold mass in the insulation vacuum of the cryostat. The temperature at this location is about 20 K. First loss measurements are expected at the end of 2015.

New 11 T dipole magnets are considered for selected locations in the LHC dispersion suppressors as part of an upgrade of the collimation system [25]. If this option is chosen, they could be equipped with cryogenic BLMs inside the magnet cold mass, and would allow for the first measurements in 1.9 K liquid helium in the LHC machine.

BACKGROUND FROM ACCELERATING STRUCTURES

Potential sources of background generated by high gradient accelerating structures are due to dark current and voltage breakdown. Dark currents are electrons which are released from internal surfaces by electron field emission and then accelerated, generating X-rays and secondary showers when they impinge on cavity walls or other beamline components. Besides RF accelerating structures, particle sources emit dark currents as well. Voltage breakdown refers to an internal discharge in the RF cavity, creating an electric arc. It is accompanied by a high emission of X-rays and electrons. In the case of the CLIC two beam module a breakdown current on the order of 100 A can occur in the main beam structure [17]. Not only do these effects limit the possibility to measure primary beam losses, they have a negative impact on the performance of the accelerator: They reduce the beam stability and/or availability, lead to component heating and radiation aging, and can result in quenches in superconducting structures. Beam loss monitors can also be employed to measure such events which are a priori not associated with beam losses, but which can easily trigger additional beam losses.

Example: CLIC Main Linac Cavity

An optical fiber Cherenkov loss monitor coupled to Multi-Pixel Photon Counter (MPPC) readout has been installed at an experiment of the CLIC Test Facility (CTF3), where a dedicated study of the performance of a loaded and unloaded CLIC accelerating structure is ongoing. The aim is to study the sensitivity limitations of the beam loss measurements and the feasibility to use such a system for RF cavity diagnostics [26]. A 900 μm core radius Cherenkov fiber was exposed over 30 cm at a distance of 2.5 cm from the structure. It was shown that both dark current and breakdown induced signals in the absence of electron beam are well within the measurement range. They have been measured as a function of cavity input power in a range of 22 MW to 34 MW and extrapolated to the nominal 40 MW and 60 MW for unloaded and loaded main beam RF structures respectively. The signals increase exponentially with the cavity input power, the dark current signal increasing much more strongly than the signal from breakdown, see Fig. 3. The extrapolation to 40 MW yields 2.2×10^5 and 5.7×10^6 detected Cherenkov photons for dark current and for RF breakdown respectively in a fiber volume of 0.76 cm^3. This indicates a very high electron background in the close vicinity of the accelerating structure and will reduce the sensitivity to low beam losses.

Example: Cryogenic Loss Monitors at Fermilab

Cryogenic Loss Monitors (CLM) [27] have been developed for Fermilab's Advanced Superconducting Test Accelerator (ASTA), a test facility for ILC-type superconducting RF acceleration structures. The purpose of the CLM is the measurement of beam losses and in particular of RF dark current induced losses. The coaxial design ionization chambers
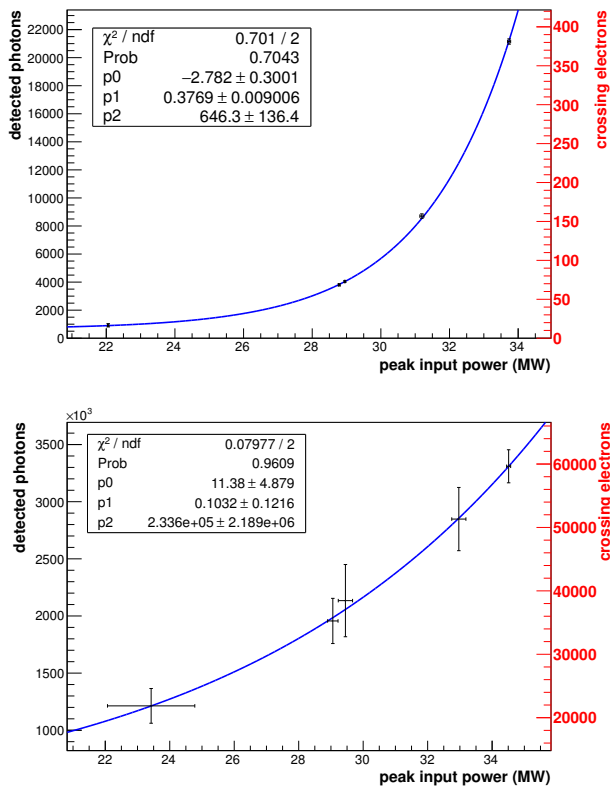
Figure 3: Signal in an optical fiber as a function of cavity input power for electron field emission (top) and RF breakdown (bottom) in number of photons detected (left y-axis). The right y-axis is an estimate of the number of electrons with $\beta = 1$ that will give the respective signal when crossing the fiber detector [26].

are filled with $120\,cm^3$ helium gas at a pressure of 1–1.5 bar. They can operate down to 5 K (and up to 350 K); as helium-4 becomes liquid below 5 K, the detectors cannot be operated at lower temperatures. The chambers are designed to be installed inside the cryomodules of RF structures and to measure dose rates of up to 300 Gy/hour with a sensitivity of approximately 0.19 nA/(Gy/hour). Dark current measurements at the A0-photo-injector test accelerator and the Horizontal Test Stand (HTS) were reported [27].

BACKGROUND FROM SYNCHROTRON RADIATION

Example: Simulation Study Comparing Different Detectors

A FLUKA simulation study was conducted recently on the sensitivity limitation of beam loss measurement in the CLIC damping ring arcs due to synchrotron light from the bending magnets [28]. The damping rings are required to reduce the transverse emittance of the electron and positron beams by synchrotron radiation damping in the superconducting wiggler magnets (2.5 T) installed in the two straight sections. The parameters of the simulation are: 2.86 GeV

electron beam energy, 200 mA current, bending field of 1 T, critical energy of the synchrotron radiation of 5.4 keV. These parameters are very similar to several existing synchrotron light sources, e. g. the Australian Synchrotron, where several test measurement campaigns for CLIC BLM have been carried out.

The worst case for synchrotron radiation background from the dipoles was investigated using a simplified geometry [28]. Typical detector types were placed close to the beamline (10 cm and 40 cm) at the location of the maximum radiation, without any shielding. LHC-type ionization chambers [29, 30], NE102 plastic scintillators ($25 \times 16 \times 2\,cm^3$) coupled to a photomultiplier tube with a gain of 10^4, silicon PIN diodes in current mode with an area of $1\,cm^2$ and a depletion layer of $100\,\mu m$, and small Cherenkov crystals with a volume of $1\,cm^3$ coupled to either a photomultiplier tube with a gain of 10^4 or an SiPM (Silicon Photomultiplier) with a gain of 10^5 were investigated. As the spectrum is not hard enough to produce electrons above the Cherenkov threshold in quartz (about 190 keV), the Cherenkov detectors are insensitive to the synchrotron radiation induced charged particle showers. Preliminary results yield, at 10 cm distance from the beampipe, currents of 80 pA, 64 µA, and 300 pA for the ionization chamber, the scintillator, and the PIN diode respectively. For the PIN diode this value is smaller than its typical dark current. The other two detectors will be able to measure the synchrotron radiation, at least when placed favorably, as in this simulation. The detector response to electron beam loss was simulated as well. For reasons of comparison the electron loss location simulated is also at the end of an arc dipole.

Figure 4 shows the resulting sensitivity limits for measuring beam losses. In red are typical values (upper and lower range) for the dark current of the respective detectors expressed in beam loss rates using the FLUKA results. They indicate the lower end of the dynamic range for measuring electron beam losses for the PIN diode and the Cherenkov crystal. Indicated in green are the beam loss rates which cannot be measured (at these locations), as their loss signal is below the signal from the synchrotron radiation. For ionization chambers and scintillators they determine the lower limit of measurable loss rates. The lowest detection limit for losses is that of the ionization chamber with 1.2×10^7 e$^-$/s. The Cherenkov counter (assuming charge multiplication at the lower end of the dark current range) and scintillator have very similar limits with 4×10^7 e$^-$/s and 3.7×10^7 e$^-$/s respectively. It is interesting to note that in this radiation field the advantage of the Cherenkov counter of being insensitive to photons is counteracted by its low sensitivity and by choosing a very small crystal size. The sensitivity limit of the Cherenkov detector decreases linearly with the increase in crystal size (not accounting for reduction in light collection efficiency, nor attenuation), as the dark current is dominated by the photon detector. At the same size as the scintillator ($800\,cm^3$), for example in the form of a quartz rod, beam loss rates down to 5×10^4 e$^-$/s could be measured. The CLIC conceptual design report [17] specifies that the
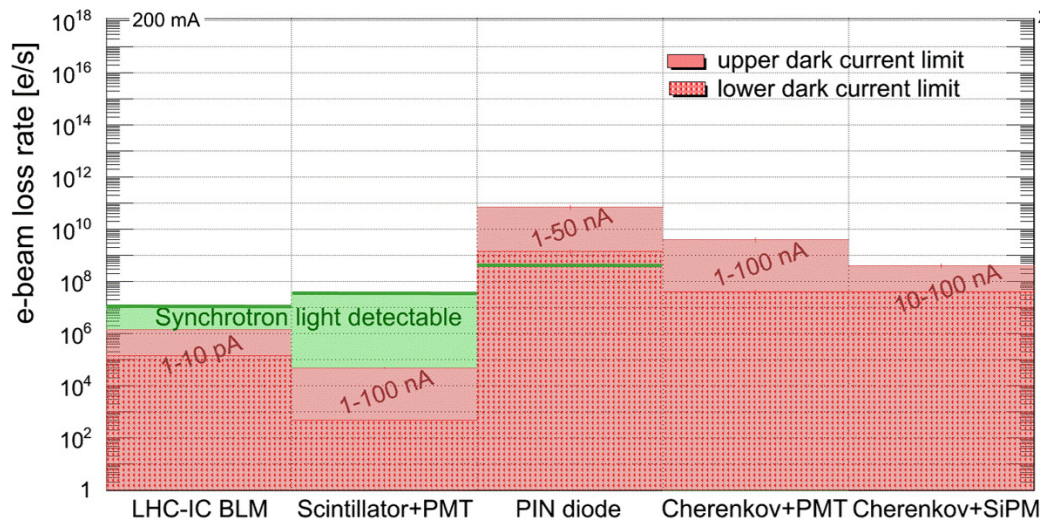
Figure 4: Worst case estimate of detector sensitivity to beam losses in the CLIC damping ring arcs based on FLUKA simulations [28].

BLM system in the damping rings should be able to measure loss rates of 2×10^7 e$^-$/s per meter. In the arcs, a Cherenkov crystal of a few cm^3 should be able to achieve this. An ionization chamber would have to be carefully positioned outside of the synchrotron radiation. In any case, exposure to synchrotron radiation should be kept low to limit radiation aging by positioning the monitors in low background regions and/or by shielding of the monitors.

Loss measurements with optical fibers at the Australian Synchrotron in the presence of synchrotron radiation have shown a sensitivity down to about 1×10^4 electrons lost in a single location using MPPC (Multi-Pixel Photon Counter) as photon detectors, and a dynamic range of 10^5 when combining MPPC at low count rate with photomultiplier readout at high count rate [31].

Example: HERA PIN Diodes

PIN diodes, albeit in counting mode, have been used very successfully in much harder synchrotron radiation backgrounds for loss measurements. The HERA machine at DESY collided protons at 920 GeV/c (from a superconducting 6.3 km proton ring) with 30 GeV/c electrons (positrons). Dual PIN diodes (mounted face-to-face) in coincidence counting mode were developed to measure proton beam losses and to provide quench protection in the presence of synchrotron radiation with a critical energy of 88 keV at a dose rate of about 10^4 Gy/year from the counter-circulating electron beam [32, 33]. The efficiency to detect a charged particle in coincidence mode was shown to be still above 30 % (compared to 70 % for a single diode). A synchrotron photon, on the other hand, only generates a signal in one of the diodes, mostly due to photoelectric absorption and due to Compton scattering for the higher photon energies. Coincidence counts due to synchrotron radiation can occur either statistically (due to high photon flux) or if the created electron has an energy high enough to reach the second

diode. The detection efficiency of photons in coincidence mode has been reported as 3.5×10^{-5}, which means excellent suppression. Lead shielding had to be applied in addition to reduce the photon count rate. The maximum count rate of 10.4 MHz corresponded to the proton bunch spacing of 96 ns. The integration time was 5.2 ms; the time resolution is limited by the relatively low count rate. A wide dynamic range of up to 10^9 was achieved as well as a good calibration. The measured beam lifetime by current decay and by beam losses agreed to within a factor of 2.

The dual coincidence counting PIN diodes were also used for loss measurements at the HERA electron ring. Here, an additional thin layer of metal between the two diodes was applied to absorb electrons created by the photons, and further reduce the background. In the meantime these detectors are commercially available, and have been/are used by several machines.

REFERENCES

[1] B. Dehning et al., "Test of a Diamond Detector Using Unbunched Beam Halo Particles", CERN-ATS-2010-027.

[2] E. Effinger et al., "A prototype readout system for the Diamond Beam Loss Monitors at LHC", IBIC 2013, Oxford, UK, MOPC45.

[3] E. Griesmayer et al., "A Fast CVD Diamond Beam Loss Monitor for LHC", Conf. Proc. C11-05-16.4 (2011), MOPD41, DIPAC 2011, Hamburg, Germany.

[4] A. Lechner et al., "Post-LS1-BLM Thresholds for the LHC Arcs," to be published in the Proc. of the Workshop on Beam Induced Quenches BIQ, CERN, Geneva, Switzerland (2014).

[5] G. Battistoni et al., "The FLUKA code: Description and Benchmarking", Proc. of the Hadronic Shower Simulation Workshop 2006, Fermilab, Batavia, USA; AIP Conference Proceeding 896, 31-49, (2007).

[6] A. Fassò et al., "FLUKA: a multi-particle transport code", CERN-2005-10 (2005), INFN/TC-05/11, SLAC-R-773.

[7] B. Auchmann et al., "Testing Beam-Induced Quench Levels of LHC Superconducting Magnets," Phys. Rev. S. T. A. B. **18** (2015) 061002 [arXiv:1502.05261 [physics.acc-ph]].

[8] T. Obina, Y. Yano, "Optical fibre based Beam Loss Monitoring for electron storage rings", IBIC 2013, Oxford, UK.

[9] X.-M. Maréchal, Y. Asano, T. Itoga, "Design, development, and operation of a fiber-based Cherenkov beam loss monitor at the SPring-8 Angstrom Compact Free Electron Laser", Nucl. Instrum. Meth. A **673** (2012) 32.

[10] L. Fröhlich et al., "Instrumentation for Machine Protection at FERMI@ELETTRA," DIPAC 2011, Hamburg, Germany.

[11] F. Wulf, M. Körfer, "Beam Loss and Beam Profile Monitoring with Optical Fibers," DIPAC 2009, Basel, Switzerland.

[12] J. W. van Hoorne, "Cherenkov Fibers for Beam Loss Monitoring at the CLIC Two Beam Module," CERN-THESIS-2012-112.

[13] M. Zingl, "Longitudinal Resolution of Cherenkov Fibers – Loss Simulations and Signal Calculation for the CLIC Drive Beam Decelerator", unpublished report.

[14] E. Nebot et al., "Position Resolution of Optical Fibre-Based Beam Loss Monitors Using Long Electron Pulses", IBIC 2015, Melbourne, Australia, WEBLA03, *these proceedings.*

[15] G. Venturini et al., "A 120 dB dynamic-range radiation-tolerant charge-to-digital converter for radiation monitoring" Microelectronics Journal 44 (2013) 1302-1308.

[16] G. Venturini et al., "Characterization of a Wide Dynamic-Range, Radiation-Tolerant Charge-Digitizer ASIC for Monitoring of Beam Losses," IBIC 2012, Tsukuba, Japan, MOPA12.

[17] M. Aicheler et al., "A Multi-TeV Linear Collider Based on CLIC Technology : CLIC Conceptual Design Report," CERN-2012-007, SLAC-R-985, KEK-Report-2012-1, PSI-12-01, JAI-2012-001.

[18] M. Kastriotou et al., "BLM Crosstalk Studies at the CLIC Two-Beam Module," IBIC 2015, Melbourne, Australia, MOPB045, *these proceedings.*

[19] O. S. Bruning et al., "LHC Design Report Vol.1: The LHC Main Ring," CERN-2004-003-V1.

[20] M. R. Bartosik et al., "Cryogenic Beam Loss Monitors for the Superconducting Magnets of the LHC," IBIC 2014, Monterey, USA; CERN-BE-2014-009.

[21] C. Kurfürst, "Cryogenic Beam Loss Monitoring for the LHC", CERN-THESIS-2013-232.

[22] C. Kurfürst et al., "In situ radiation test of silicon and diamond detectors operating in superfluid helium and developed for beam loss monitoring," Nucl. Instrum. Meth. A **782** (2015) 149.

[23] A. F. Borghesani, *Ions and Electrons in Liquid Helium,* Print ISBN-13: 9780199213603, Oxford Science Publications (2007); DOI:10.1093/acprof:oso/9780199213603.001.0001 Oxford Scholarship Online (2008).

[24] M. R. Bartosik et al., "Cryogenic Beam Loss Monitors for the Superconducting Magnets of the LHC," IBIC 2015, Melbourne, Australia, MOPB042, *these proceedings.*

[25] N. Andreev et al., "Design and Fabrication of a Single-Aperture 11T Nb_3Sn Dipole Model for LHC Upgrades," IEEE Trans. Appl. Supercond. **22** (2012) 3, 4001705.

[26] M. Kastriotou, "RF cavity induced sensitivity limitations on Beam Loss Monitors," LA3NET 2015, Phys. Procedia (2015) accepted.

[27] A. Warner, J. Wu, "Cryogenic loss monitors with FPGA TDC signal processing," Phys. Procedia **37** (2012) 2031.

[28] S. Damjanovic, to be published.

[29] E. B. Holzer et al., "Development, Production and Testing of 4500 Beam Loss Monitors," EPAC 2008, Genoa, Italy, Conf. Proc. C **0806233** (2008) TUPC037; CERN-AB-2008-054.

[30] E. B. Holzer et al., "Beam loss monitoring system for the LHC," NSS 2005, IEEE Transactions on Nuclear Science, Vol. 53 (2006) p.1052; CERN-AB-2006-009.

[31] E. Nebot et al., "Measurement of Beam Losses Using Optical Fibers at the Australian Synchrotron", IBIC 2014, Monterey, USA.

[32] K. Wittenburg, "The PIN-diode beam loss monitor system at HERA," BIW 2000, Cambridge, Massachusetts, USA; DESY-HERA-00-03.

[33] K. Wittenburg, "Preservation of beam loss induced quenches, beam lifetime and beam loss measurements with the HERAp beam-loss-monitor," Nucl. Instrum. Meth. A **345** (1994), 226.